Slow Second-Order Reactions in a Deflected Buoyant Jet

An integral method including the entrainment hypothesis of Hoult, Fay and Forney (1969) is used to predict the concentration of product formed in a buoyant jet in a crossflow. The analysis is restricted to a slow, irreversible, second-order reaction with premixed reactants. Reliable laboratory data are presented for the oxidation of nitric oxide by the reaction $2NO + O_2 \rightarrow 2NO_2$ with excess O_2 and these results are correlated with the theory. Additional measurements are recorded to provide information on the magnitude of the turbulent parameters necessary for proper closure of the rate expressions.

L. J. FORNEY and L. A. OAKES

School of Chemical Engineering
Georgia Institute of Technology
Atlanta, GA 30332

SCOPE

Most important chemical reactions in industry are promoted with turbulence. Turbulent mixing creates small contiguous masses of reactant species or eddies which reduce the necessary time for molecular mixing and reaction on the scale of the eddy size. A general review of turbulent mixing in chemically reactive flows is provided by Brodkey (1975). A common method of mixing fluids for the purpose of promoting chemical reactions is to use turbulent jets. Fluid jets play an important role in pipe mixing, combustion, jet mixing in tanks or reactors and the dilution of toxic by-products from power plants and other industrial operations. Recent reviews of the mechanics of jet behavior of all kinds are given by Rajaratnam (1976) and Fischer et al. (1979).

Investigations of chemically reactive flows within turbulent jets have been largely confined to studies of fully developed turbulent jets in a stagnant or coaxial flowing ambient fluid. Examples of several studies which treat this problem are those of Gouldin (1974), Lin and O'Brien (1974), McKelvey et al. (1975), Singh and Toor (1975), and Toor (1975). The turbulent properties of simple axisymmetric jets in a stagnant environment are well established. The flow fields are self-similar and several theoretical approaches such as dimensional considerations, similarity analyses, Prandtl mixing length arguments and several entrainment hypotheses can be used to correlate empirical results (Rajaratnam, 1976).

It is common, however, to employ turbulent jets in an ambient crossflow. Deflected jets of this nature, which dilute more rapidly than jets without crossflows, are not axisymmetric or uniformly self-similar. Theoretical approaches in this case are restricted to integral methods of the type proposed by Morton, Taylor and Turner (1956) or to simple dimensional arguments. A complete review of the problem is given by Wright (1977). Deflected jets are further complicated if they are buoyant relative to the ambient crossflow. In this case the jet's trajectory and dilution rate are dominated by momentum in the near-field, buoyancy in the far-field and an intermediate transition region. Moreover, the physical extent of each of these regimes, may be difficult to predict (Fischer et al., 1979).

In this paper, an integral method including the entrainment hypothesis developed by Hoult, Fay and Forney (1969) is used to predict the concentration of product formed in a buoyant jet in a crossflow. The analysis is restricted to a slow, irreversible, second-order reaction with premixed reactants. Reliable laboratory data are presented to correlate the theoretical predictions and to provide information on the magnitude of the turbulent parameters necessary for proper closure.

CONCLUSIONS AND SIGNIFICANCE

The progress of a slow, irreversible, second-order reaction in a buoyant jet in a crossflow with premixed reactants has been investigated. Analytical expressions for the product of a bimolecular reaction of the form $A + B \rightarrow AB$ are derived, valid for $[AB]/[A] \ll 1$ and the ratio of momentum-to-buoyancy length $l_m/l_b \sim 0(1)$. The results indicate that the reaction is quenched, with a shift in importance from far to near-field kinetics as the initial buoyancy flux increases or $l_m/l_b \rightarrow 0$. A correction factor is provided for the analytical result by comparison with numerical solutions to the conservation expressions over the range $10^{-2} < l_m/l_b < 10^2$. A perturbation expansion demonstrates that the limiting conversion ratio sharply decreases with increasing buoyancy flux such that $[AB]/[A] \sim (l_m/l_b)^{g(\lambda)}$ where $1.0 < g(\lambda) < 1.2$.

Experimental measurements of the oxidation of nitric oxide by the reaction $2NO + O_2 \rightarrow 2NO_2$ in a low-speed wind tunnel indicate excellent agreement with theory. In addition, measurements of methane dilution provide empirical values for the turbulent parameters necessary for closure of the rate expression used in the analysis.

INTRODUCTION

Attempts to predict the progress of chemical reactions in turbulent flows are difficult. From a practical standpoint, however, there are two asymptotic cases involving chemically reactive species in turbulent flow fields that lend themselves to an analytical treatment. For example, if the chemical reaction times are much smaller than characteristic time scales associated with molecular diffusion, the progress of the reaction is diffusion-limited. In the opposite case, when the reaction time is very long compared to the mixing time, one has a kinetically limited reaction. For proper closure of the conservation expressions in the diffusion-limited case, additional experimental and theoretical information is inevitably necessary concerning the magnitude of the turbulent fluctuating components. In general, slow kinetically limited reactions are simpler to analyze than the fast diffusion-controlled case since one

can neglect the turbulent fluctuating components.

An early attempt to include fast chemical reactions in a deflected jet is that of Escudier (1972) who used the integral method of Hoult, Fay and Forney (1969) to study the effect of heat release on the jet trajectory during combustion. More recently, Forney and Giz (1981) used the same integral method to consider fast reversible reactions in a buoyant jet in a crossflow. Slow second-order reactions were used in Gaussian plume models by Schwartz and Newman (1978) and Freiberg (1978) with potential application to the chemistry of effluents from power plants. Integral methods were used on the problem of slow reactions in deflected buoyant jets by Forney and Giz (1980), who studied reactions of arbitrary order and Heffner (1981), who considered the effect of the entrainment of one reactant on the progress of a third-order reaction.

In all of the previous work involving the application of integral methods to reactions in turbulent jets in a crossflow, the turbulent fluctuating components have been neglected and it has been assumed that the reactants are uniformly distributed for a given jet cross section. In the present paper, the turbulent fluctuating components are neglected, which is justified for the slow, kinetically limited reaction considered, but proper attention is now given to the spatial distribution of the reactant concentrations. In addition, the analytical results are correlated with the first reliable laboratory data.

THEORY

The integral method used in this work to predict the trajectory and growth of a turbulent buoyant jet in a laminar crossflow was originally proposed by Hoult, Fay and Forney (1969). The theory represents an extension to the entrainment hypothesis or local similarity ideas first advanced by Morton, Taylor and Turner (1956) to analyze properties of vertical plumes in a stationary ambient fluid. In the model, the rate of entrainment is assumed to be proportional to the product of the local jet transverse length scale and the tangential and normal velocity difference between the jet and the surrounding fluid. Two constants of proportionality or entrainment parameters are used in the model to account for the linear combination of entrainment rates due to each velocity difference. A complete description of the model and its application to laboratory and field measurements is given by Forney (1968), Hoult, Fay and Forney (1969), Hoult and Weil (1972), and Fay (1973).

Rate Expression

In this paper we consider a slow, irreversible, bimolecular reaction of the form

$$A + B \xrightarrow{k} AB \tag{1}$$

where the reactants are premixed or self-contained at the jet exit. Referring to Figure 1, we assume for simplicity that the jet is axisymmetric and write the conservation expression for the product AB

$$u_s \frac{\partial [AB]}{\partial s} + u_r \frac{\partial [AB]}{\partial r} = -\frac{1}{r}\frac{\partial}{\partial r}\left(r \overline{u_r' [AB]'}\right) + k([A][B] + \overline{[A]'[B]'}). \tag{2}$$

Here, $[A]$, $[A]'$ are, respectively, the local time-averaged and turbulent fluctuating concentration components; u_s, u_r are the local time-averaged axial and radial jet velocities; and the overbars represent temporal averages.

Neglecting the reactant turbulent fluctuating component or assuming $\overline{[A]'[B]'}/[A][B] \ll 1$, we multiply Eq. 2 by r and integrate over the cross-sectional area of the jet. It can be shown (Wright, 1977) that Eq. 2 reduces to

$$\frac{d}{ds}\int u_s [AB] d\mathcal{A} = k \int [A][B] d\mathcal{A}. \tag{3}$$

Integrating Eq. 3 over the jet cross-sectional area as indicated, without making assumptions concerning the shape of the profiles of jet properties, the conservation expression for species AB reduces to

$$\frac{d}{ds}(u[\overline{AB}]b^2) = k \int [A][B] d\mathcal{A} \tag{4}$$

Here in Eq. 4 and in the following discussion, the overbars represent bulk mean values for the concentrations, u is the characteristic jet velocity, and b is the transverse length scale where

$$[\overline{A}] = \frac{\int u_s [A] d\mathcal{A}}{\int u_s d\mathcal{A}} \tag{5}$$

$$u = \frac{\int u_s^2 d\mathcal{A}}{\int u_s d\mathcal{A}} \tag{6}$$

and

$$\pi b^2 = \frac{(\int u_s d\mathcal{A})^2}{\int u_s^2 d\mathcal{A}}. \tag{7}$$

We now restrict the reaction rate to slow reactions such that $[AB]/[A] \ll 1$ everywhere in the jet flow field. This implies that the reactants A and B of Eq. 1 are approximately conserved in the jet. Closure is then accomplished by defining a parameter

$$1/\gamma = \frac{\int [A][B] d\mathcal{A}}{\pi b^2 [\overline{A}][\overline{B}]} \tag{8}$$

representing the ratio of the indicated bulk mean reactant concentrations where γ is assumed to be a constant along the axis of the jet and determined by experiment. Substituting for γ in Eq. 4, the rate expression for the product AB is written in the form

$$\frac{d}{ds}(u\,[\overline{AB}]b^2) = \frac{k}{\gamma}[\overline{A}][\overline{B}]b^2. \tag{9}$$

Conservation Equations

We now consider the conservation equations for a slow bimolecular reaction within a turbulent buoyant jet in a laminar crossflow as indicated in Figure 1. It is assumed that the jet is directed parallel to the gravitational force and perpendicular to the crossflow. The jet is also considered to be in hydrostatic equilibrium with the ambient fluid and to have a mean exit velocity u_o which exceeds the crossflow velocity v such that $u_o/v \gtrsim 1.2$. The latter restriction insures that the jet trajectory is free of its wake. For simplicity, we also make the Boussinesq approximation or $|\rho_\infty - \rho_o|/\rho_o \ll 1$. With these assumptions, the conservation equations for the buoyant jet can be written in the form indicated below (Hoult, Fay and Forney, 1969).

Conservation of mass:

$$\frac{d}{ds}(b^2 u) = 2b[\alpha|u - v\cos\theta| + \beta|v\sin\theta|] \tag{10}$$

Conservation of tangential momentum:

$$\frac{d}{ds}(b^2u^2) = b^2 g \sin\theta\left(\frac{\rho_\infty - \rho}{\rho_o}\right) + v\cos\theta\frac{d}{ds}(b^2u) \tag{11}$$

Conservation of normal momentum:

$$b^2u^2\frac{d\theta}{ds} = b^2 g\cos\theta\left(\frac{\rho_\infty - \rho}{\rho_o}\right) - v\sin\theta\frac{d}{ds}(b^2u) \tag{12}$$

Conservation of buoyancy:

$$\frac{d}{ds}\left[b^2 u\left(\frac{\rho_\infty - \rho}{\rho_o}\right)\right] = 0 \tag{13}$$

Conservation of species:

$$\frac{d}{ds}(u[\overline{AB}]b^2) = \frac{k}{\gamma}[\overline{A}][\overline{B}]b^2 \tag{14a}$$

and

$$\frac{d}{ds}(u[\overline{A}]b^2) = \frac{d}{ds}(u[\overline{B}]b^2) = 0. \tag{14b}$$

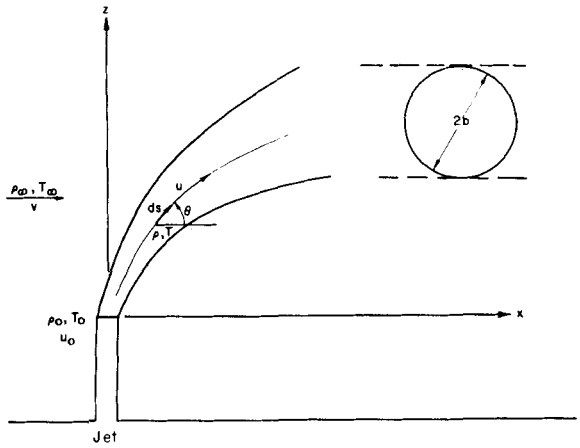

Figure 1. Schematic of a buoyant jet in a crossflow.

Equations 11–14 are subject to the initial conditions $s = 0$, $u = u_o$, $b = b_o$, $\rho = \rho_o$, $\theta = \pi/2$, $[\overline{A}] = [A]_o$, $[\overline{B}] = [B]_o$ and $[\overline{AB}]_o = 0$ where s is the distance measured along the jet axis, b is proportional to the jet radius, u is the characteristic jet velocity, v is the crossflow speed, α and β are constant entrainment parameters, and θ is the jet angle measured from the x-axis. The jet coordinates x,z, Figure 1, are computed from the geometric relations

$$\frac{dz}{ds} = \sin\theta, \frac{dx}{ds} = \cos\theta. \tag{15}$$

Asymptotic Approximations

It is not possible to find general analytical solutions to the conservation equations (Eqs. 10–15). However, useful asymptotic results can be found in the near and far field by integrating the conservation expressions along the jet axis with the constraint that the progress of the reaction is sufficiently slow so that the reactant species are approximately conserved. We also assume for simplicity in the discussion that follows that the buoyant force acts in the positive z direction away from the jet exit. Although the jet trajectory would change significantly if the buoyant force acted in other directions, the rate of growth and thus the progress of the chemical reaction would change little.

Assuming an initial mass, momentum and buoyancy flux at the jet exit, one normally encounters three distinct regimes of jet trajectory and growth, as described by Hoult and Weil (1972) and Fischer et al. (1979). Although, in principle, it would be possible to derive approximate expressions for the progress of the chemical reaction in each of the regimes, the mathematics would be cumbersome. Moreover, the boundary conditions or physical extent of each regime depend strongly on empirically determined coefficients and few empirical data exist for the coefficients which appear in the jet growth laws. There are three limiting cases, however, that involve only two regimes for jet growth. Two of these cases result from either a negligible initial momentum or buoyancy flux which would not be useful in the present application. If there is an initial momentum and buoyancy flux, however, and we assume that the momentum and buoyancy lengths which scale the jet properties in the near and far field are similar in magnitude or $l_m/l_b \sim 0(1)$, jet growth can be described with just two regimes. Therefore, we find it convenient in the discussion that follows to derive approximate expressions for the limiting case of $l_m/l_b \sim 0(1)$ which is common in practical applications where l_m and l_b are defined below.

Near-Field Solutions ($x < l_m$). Close to the jet exit where $s \to 0$, $\theta \to \pi/2$ and $z \to s$ one can show from Eqs. 10, 11 and 13 that to first order (Forney and Kwon, 1979; Forney and Giz, 1980; Forney and Heffner, 1982)

$$\frac{b^2u}{b_o^2u_o} = \frac{[A]_o}{[A]} = 1 + ay \tag{16}$$

and

$$\frac{u_o}{u} = \frac{1 + ay}{1 + cy}, \tag{17}$$

where $y = s/l_b = z/l_b$, $a = 2(\eta^2/R)(l_b/l_m)$, $c = 1/R\,(l_b/l_m)^2$, $R = u_o/v$ and $\eta = [R(\alpha R + \beta)]^{1/2}$. Here, $\alpha(= 0.11)$ and $\beta(= 0.6)$ are constant entrainment parameters determined from laboratory measurements, $l_m(= b_oR)$ is the momentum length, $l_b(= F_o/v^3)$ is the buoyancy length where $F_o = u_ob_o^2g|\rho_\infty - \rho_o|/\rho_o$. Moreover, $[A]$ is the bulk mean value of the jet concentration where the overbars used before have been dropped for convenience in the discussion that follows. Since the jet trajectory in the near field (Hoult, Fay and Forney, 1969) is:

$$z/l_m = (R/\eta)(x/l_m)^{1/2}, \tag{18}$$

the quantity $ay = \Omega(x/l_b)^{1/2}$ in Eq. 17 if $\Omega = 2\eta(l_b/l_m)^{1/2}$. When $x \to l_m$ it should be noted in Eqs. 16–18 that $z/l_m = R/\eta$ and $ay = 2\eta$.

Substituting Eqs. 16–18 into Eq. 14a and integrating with the boundary conditions $s = 0$, $[A] = [A]_o$, $[B] = [B]_o$ and $[AB] = [AB]_o = 0$, one has for the concentration of product AB,

$$\frac{[AB]}{[A]_o} = \frac{kl_b[B]_o}{vR\gamma}\left(\frac{1}{1 + \Omega(x/l_b)^{1/2}}\right)\int_o^y \frac{dy}{1 + cy} \tag{19}$$

or for $x < l_m$,

$$\frac{[AB]}{[A]_o} = \frac{kl_b[B]_o}{v\gamma}\left(\frac{l_m}{l_b}\right)^2\left(\frac{1}{1 + \Omega(x/l_b)^{1/2}}\right) \cdot \ln\left[1 + \frac{1}{\eta}\left(\frac{l_b}{l_m}\right)^{3/2}\left(\frac{x}{l_b}\right)^{1/2}\right] \tag{20}$$

where the fractional conversion ratio derived from Eqs. 16 and 20 is

$$\frac{[AB]}{[A]} = \frac{kl_b[B]_o}{v\gamma}\left(\frac{l_m}{l_b}\right)^2 \ln\left[1 + \frac{1}{\eta}\left(\frac{l_b}{l_m}\right)^{3/2}\left(\frac{x}{l_b}\right)^{1/2}\right]. \tag{21}$$

Far-Field Solutions ($x > l_b$). In the far field where $s \to x, u \to v$ and $\theta \to 0$, one can show (Hoult, Fay and Forney, 1969; Forney and Giz, 1980) for the conservation of A

$$\frac{[A]}{[A]_o} = R\left(\frac{b_o}{b}\right)^2 = \frac{1}{R}\left(\frac{l_m}{l_b}\right)^2\left(\frac{2}{3\beta}\right)^{2/3}\left(\frac{x}{l_b}\right)^{-4/3}. \tag{22}$$

Neglecting a transition region for $x > l_m$ as discussed earlier, we now assume for simplicity that Eq. 22 applies for all $x > l_m$. Substituting Eq. 22 into Eq. 14a and integrating where $y = x/l_b$ one has

$$\frac{[AB]}{[A]_o} = \frac{kl_b[B]_o}{v\gamma}\left(\frac{1}{R^2}\right)\left(\frac{l_m}{l_b}\right)^4\left(\frac{2}{3\beta}\right)^{4/3}\left(\frac{x}{l_b}\right)^{-4/3}\int_{l_m/l_b}^{y} y^{-4/3}\,dy. \tag{23}$$

If $x/l_b \gg 1$, the far-field contribution Eq. 23 becomes

$$\frac{[AB]}{[A]_o} = \frac{kl_b[B]_o}{v\gamma}\left(\frac{1}{R^2}\right)\left(\frac{l_m}{l_b}\right)^{11/3}\left(\frac{16}{3\beta^4}\right)^{1/3}\left(\frac{x}{l_b}\right)^{-4/3} = \Delta_1. \tag{24}$$

Account must now be taken of the product AB as described in Eq. 20. This product is formed in the near field over the distance $0 < x < l_m$ and subsequently dilutes in the far field. Since continuity yields $[AB]b^2v = ([AB]b^2u)_{x=l_m}$, the component of the total AB in the far field, resulting from the diluted near-field contribution, becomes

$$\frac{[AB]}{[A]_o} = \left(\frac{b_o^2u_o}{b^2v}\right)\left[\frac{[AB]}{[A]_o}\left(\frac{b^2u}{b_o^2u_o}\right)\right]_{x=l_m} \tag{25}$$

or, substituting with Eqs. 16, 20 and 22, one has

$$\frac{[AB]}{[A]_o} = \frac{kl_b[B]_o}{vR\gamma}\left(\frac{2}{3\beta}\right)^{2/3}\left(\frac{l_m}{l_b}\right)^4\left(\frac{x}{l_b}\right)^{-4/3}\ln\left[1 + \frac{1}{\eta}\left(\frac{l_b}{l_m}\right)\right] = \Delta_2. \tag{26}$$

Combining Eqs. 24 and 26 for the total AB formed in the far-field $x/l_b \gg 1$, one has

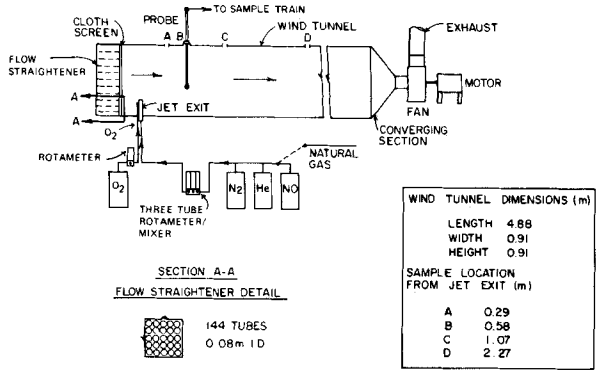

Figure 2. Schematic of the low-speed wind tunnel.

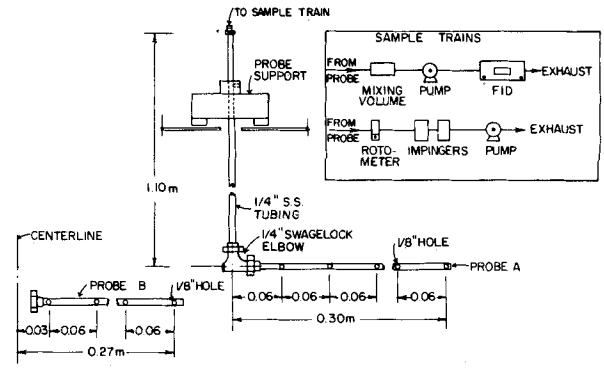

Figure 3. Sample probe used in wind tunnel.

$$\frac{[AB]}{[A]_o} = \frac{kl_b[B]_o}{v\gamma}\left(\frac{1}{R^2}\right)\left(\frac{l_m}{l_b}\right)^{11/3}\left(\frac{16}{3\beta^4}\right)^{1/3}\left(\frac{x}{l_b}\right)^{-4/3}\left(1+\frac{\Delta_2}{\Delta_1}\right). \quad (27)$$

Here,

$$\frac{\Delta_2}{\Delta_1} = R\left(\frac{\beta^2}{12}\right)^{1/3}\left(\frac{l_m}{l_b}\right)^{1/3}\ln\left[1+\frac{1}{\eta}\left(\frac{l_b}{l_m}\right)\right] \quad (28)$$

represents the relative contributions of the near field (Δ_2) and far field (Δ_1) to the product concentration $[AB]$ when $x/l_b \gg 1$ from Eqs. 24 and 26. Dividing Eq. 27 by Eq. 22, the conversion ratio in the far field $x/l_b \gg 1$ now becomes

$$\frac{[AB]}{[A]} = \frac{kl_b[B]_o}{v\gamma}\left(\frac{1}{R}\right)\left(\frac{l_m}{l_b}\right)^{5/3}\left(\frac{12}{\beta^2}\right)^{1/3}\left(1+\frac{\Delta_2}{\Delta_1}\right). \quad (29)$$

This expression demonstrates that the limitation of slow reactions or $[AB]/[A] \ll 1$ implies that the jet travel time must be much less than the characteristic chemical reaction time or

$$\frac{kl_b[B]_o}{v} \ll 1.$$

EXPERIMENTAL PROCEDURE

Wind tunnel measurements were made on the progress of a slow, irreversible, second-order reaction. The reaction chosen was the slow thermal oxidation of nitric oxide to nitrogen dioxide or

$$2NO + O_2 \xrightarrow{k_o} 2NO_2. \quad (30)$$

Under conditions of excess oxygen, the rate expression for this reaction reduces to a form which is identical to that of Eq. 14a. If the product and reactant concentrations refer to bulk mean values, the rate expression is of the form

$$\frac{d}{ds}(u[NO_2]b^2) = \frac{k}{\gamma}b^2[NO]^2. \quad (31)$$

Here, $k = 2k_o[O_2]_\infty$ where $k_o = 1.3 \times 10^{-11}$ ppm^{-2} s^{-1} and the initial concentration of oxygen at the jet exit is approximately equal to its ambient value of $[O_2]_\infty = 0.21 \times 10^6$ ppm. Thus, the rate constant k in Eq. 31 reduces to a value of 5.46×10^{-6} ppm^{-1} s^{-1}.

Wind Tunnel

The experimental facility used in this work is a low-speed wind tunnel, 4.9 m in length, designed for laminar flow of uniform constant velocity air through a 91 cm^2 cross section. The wind tunnel entrance section consists of thin-walled cardboard tubes or flow straighteners, roughly 7.5 cm in diameter by 32 cm in length, arranged in a 12 by 12 array to cover the tunnel entrance, Figure 2. Behind the straightening vanes is a cloth screen consisting of several layers of loosely-packed fibrous filter-type material which suppresses turbulence and reduces the air velocity (Heffner, 1981; Oakes, 1981).

Gases were injected into the laminar crossflow through a tube, 1.5 cm in diameter by 14.7 cm in length, inserted through the floor of the tunnel approximately 15 cm downstream from the entrance. A wire mesh was inserted 1 cm below the jet exit to break up abnormal velocity profiles and assure turbulent flow. Samples were taken of jet concentrations using 0.635 cm stainless-steel tubing inserted through holes along the centerline of the tunnel roof, Figures 2 and 3. Both the front wall, made of plexiglass, and the back wall of the tunnel are ruled in centimeters at each sampling location so that the vertical position of the probe may be determined to within ±0.1 cm. Sampling holes, 0.318 cm in diameter, located along the horizontal arm of the sample probe were used to determine jet concentrations for an array of points. In this study, the sampling points were located in rows and columns 3 cm apart such that each point represented the average concentration for a sample area of 9 cm^2.

Measurements of NO Oxidation

The objective of the experimental effort was to measure values of the conversion ratio of nitrogen dioxide to nitric oxide concentration within the jet downstream from the source. Since the theory is written in terms of bulk mean concentrations, it was necessary to determine special concentration profiles of both the reactant NO and product NO_2. Because of probe size and the intermittant nature of the turbulent jet, it was impractical to make measurements in the near field. Therefore, all of the experiments in this study were conducted on the jet after it had bent over in the crossflow. Jet exit conditions of momentum-to-buoyancy length ratio l_m/l_b and velocity ratio R were prescribed with appropriate jet mixtures of helium for buoyancy, compressed air for oxygen and N_2. Complete details of this procedure are given by Heffner (1981) and Oakes (1981).

Two types of measurements were necessary in this study. The first consisted of the measurement of concentration profiles of an inert gas downstream from the jet exit. This provided useful information concerning the magnitude of the turbulent parameter γ and the rate of dilution of the reactant NO. Since nitric oxide concentrations are difficult to measure, we found that it was convenient to use a gas mixture of roughly 10^4 ppm of natural gas (referred to as CH_4) for the dilution measurements. This mixture, diluted to $\sim 5 \times 10^2$ ppm at sample port B of Figure 2, was measured with a flame ionization detector shown in Figure 3. Concentration fluctuations of CH_4 were damped at each measurement point with a 3.8 L mixing volume for a typical 4 min sample period. Concentrations of <1% of the maximum measured value were discarded and the remaining data defined the effective cross sectional area of the jet.

Concentration profiles of NO_2, the product of the slow reaction, were determined in the second series of measurements. With a typical initial nitric oxide concentration of $\sim 4 \times 10^3$ ppm, an array of NO_2 concentrations of ~0.5 ppm were measured with the Saltzman technique at sample port B of Figure 2. In this case, each sample point required up to 16 min for sufficient absorption of NO_2 in the fritted bubblers (impingers) shown in Figure 3. Values of NO_2 concentration which were less than 1 pphm, the background level, were discarded.

Data Analysis

The dilution of the reactant NO was simulated with methane. Bulk mean values of the expected concentration of NO downstream from the source were determined for given jet exit conditions from the relation

$$\frac{[NO]}{[NO]_o} = \frac{[CH_4]}{[CH_4]_o} = \frac{q}{v\mathcal{A}} \quad (32)$$

where $\mathcal{A} = \Sigma_i \Delta\mathcal{A}_i$ was evaluated from the measured grid and $q = \pi b_o^2 u_o$ is the initial volume rate of flow of the jet.

Values of the turbulent parameter $\gamma = \overline{([CH_4])^2}/\overline{[CH_4]}^2$ were determined from each array of data points where the bulk mean quantities appearing in the numerator and denominator are defined as

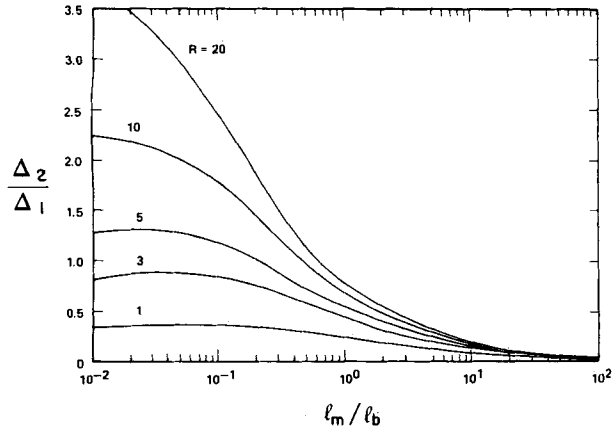

Figure 4. Ratio of near field Δ_2 to far field Δ_1 contribution to the end-point conversion ratio $[AB]/[A]$ for $x/l_b \gg 1$.

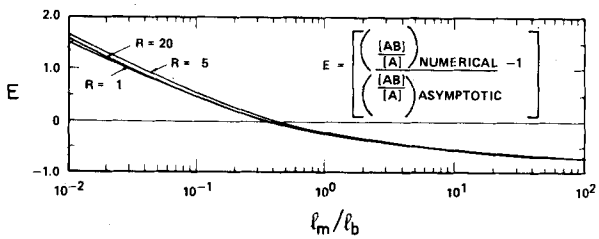

Figure 5. Relative error in the conversion ratio for $x/l_b \gg 1$.

$$(\overline{[CH_4]})^2 = \frac{1}{\mathcal{A}^2}\left(\sum_i [CH_4]_i \, \Delta\mathcal{A}_i\right)^2 \tag{33}$$

and

$$\overline{[CH_4]^2} = \frac{1}{\mathcal{A}} \sum_i [CH_4]_i^2 \, \Delta\mathcal{A}_i. \tag{34}$$

The bulk mean values of the concentration of product NO_2 were computed from the array of impinger data in the same manner as in Eq. 33. Here, we note that the definition of γ and the bulk concentrations in Eqs. 33 and 34 are simplified in the far field since $u_s \to v$.

RESULTS AND DISCUSSION

The approximate expression, Eq. 29, representing the conversion ratio $[AB]/[A]$ at long distances from the source $x/l_b \gg 1$, is formally valid when the momentum and buoyancy are roughly equal or $l_m \sim l_b$. To provide an asymptotic solution which is useful for cases where the momentum length l_m is either much larger or smaller than the buoyancy length l_b, Eq. 29 was compared with numerical solutions to the conservation equations and the comparison provided a simple correction factor to the asymptotic expression. The tacit assumption in this procedure was that the numerical solution to the conservation expressions of Eqs. 10 to 15 compared favorably with existing experimental data of Hoult and Weil (1972) and Wright (1977). This assumption was consistent with our computations.

Theory

The relative contribution of the near field Δ_2 and far field Δ_1 to the product concentration $[AB]$ at long distances from the source when $x/l_b \gg 1$ is shown in Figure 4. Here, contours of constant velocity ratio R are plotted from Eq. 28. Figure 4 demonstrates that the near-field, momentum-dominated region $x < l_m$ is largely responsible for the formation of the product AB as the buoyancy flux increases or $l_m/l_b \to 0$. If $l_m/l_b > 1$, most of the reaction occurs within the jet after it has bent over in the crossflow when $x > l_m$.

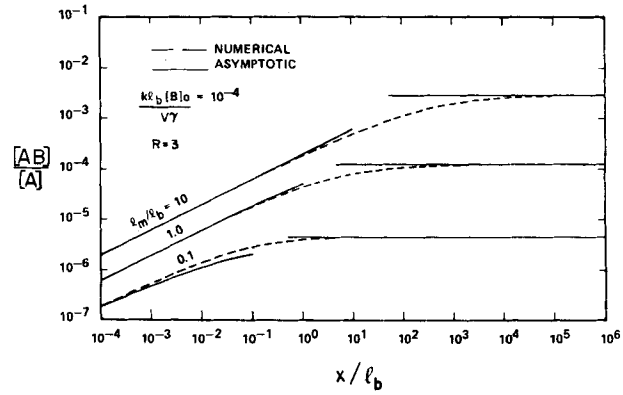

Figure 6. Conversion ratio vs. distance from jet exit. Solid lines are Eq. 21 for $x/l_m < 1$ and Eq. 36 for $x/l_b \gg 1$.

Physically, the jet entrains ambient fluid more rapidly in the far field with a larger buoyancy flux at the orifice when $l_m/l_b \to 0$ as shown in Eq. 22. Since the jet velocity perpendicular to the crossflow increases as $l_m/l_b \to 0$, the jet dilutes more rapidly resulting in a lower reactant concentration in the far field and a suppression of the chemical reaction.

The relative error between numerical solutions to the conservation equations for the total product AB formed in the far field, and the approximate expression Eq. 29 was determined for a range of momentum-to-buoyancy length ratios $10^{-2} < l_m/l_b < 10^2$ and the results are indicated in Figure 5. The error in Eq. 29 results from the inaccuracies in the asymptotic expressions used in the development of the approximation as $x \to l_m$ and from the neglect of a transition region in the far field $x > l_m$.

An empirical correction factor for Eq. 20 was developed from Figure 5. It was found that the second-order polynomial of the form

$$f(l_g) = 0.79 - 0.566 l_g + 0.144 l_g^2 \tag{35}$$

where $l_g = \log_{10}(l_m/l_b)$ reduces the relative error between Eq. 29 and the numerical solutions to less than 5%. The corrected conversion ratio in the far field $x/l_b \gg 1$ becomes

$$\frac{[AB]}{[A]} = \frac{f k l_b [B]_o}{v\gamma}\left(\frac{1}{R}\right)\left(\frac{l_m}{l_b}\right)^{5/3}\left(\frac{12}{\beta^2}\right)^{1/3}\left(1 + \frac{\Delta_2}{\Delta_1}\right) \tag{36}$$

where Δ_2/Δ_1 is defined by Eq. 28 and f is given by Eq. 35.

Contours of the conversion ratio $[AB]/[A]$ are plotted in Figure 6 for constant l_m/l_b as a function of distance from the source x/l_b. Equation 21 indicates that near the source $x/l_b \ll 1$, the conversion ratio $[AB]/[A] \sim x^{1/2}$. Far from the source for $x/l_b \gg 1$, however, the conversion ratio reaches a constant value independent of distance. The latter feature is apparent from Eqs. 29 and 36 and Figure 6. One concludes that second order reactions are ultimately quenched in the far field as the result of rapid reactant dilution.

Contours of the far field, normalized conversion ratio $[AB]/[A]$ are determined from Eq. 36 for a constant velocity ratio R as shown in Figure 7. It is clear that the progress of the chemical reaction is severely inhibited as the flux of buoyancy increases at the jet exit. Because increased buoyancy leads to a more rapid rate of entrainment of ambient fluid, the reactant concentration is diluted more quickly and the reaction is quenched closer to the source as discussed earlier. It is also shown in the Appendix that the conversion ratio, represented by Eq. 36, increases with the ratio of momentum-to-buoyancy length such that

$$\frac{[AB]}{[A]}\left(\frac{u_o\gamma}{k l_b [B]_o}\right) \sim h(\lambda)(l_m/l_b)^{g(\lambda)} \tag{37}$$

where $h(\lambda) = 2.53\,(1 + .31\,\lambda)$, $g(\lambda) = 1.35\,(1 + 0.16\,\lambda)/(1 + 0.31\,\lambda)$ and $\lambda = (\alpha + \beta/R)^{-1/2}$. Equation 37, valid in the limit as $l_m/l_b \to 1$, can be shown to represent Eq. 36 to within 2% over the range $0.1 < l_m/l_b < 10$.

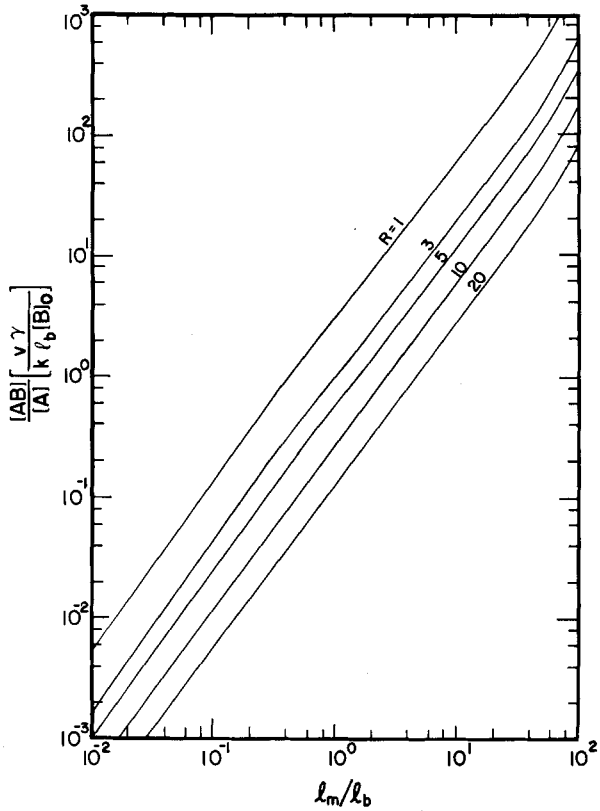

Figure 7. Contours of the normalized, end-point conversion ratio Eq. 36 for $x/l_b \gg 1$.

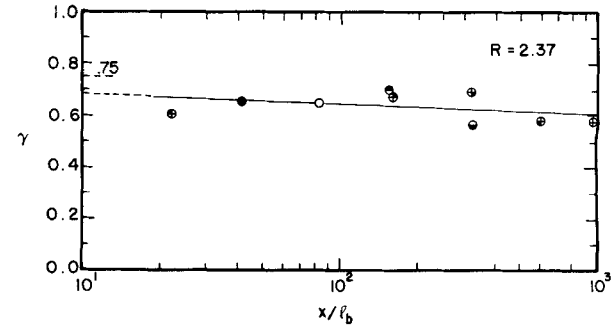

Figure 8. Plot of γ defined by Eq. 8 vs. distance from the jet exit where *A* and *B* are self-contained in the jet. The key to the symbols used is given in Table 2.

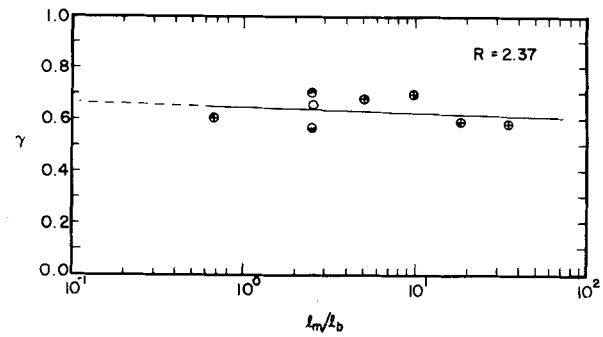

Figure 9. Plot of γ vs. the ratio of momentum-to-buoyancy length. The key to symbols used is given in Table 2.

Experiment

Two types of wind tunnel measurements were conducted for a range of jet exit conditions $0.67 < l_m/l_b < 35.0$ at fixed velocity ratio $R = 2.37$. The objective of these experiments was to determine far-field values for both the conversion ratio $[NO_2]/[NO]$ for the slow thermal oxidation of nitric oxide and the parameter γ. The first series of measurements were made to determine necessary bulk mean properties of the concentration distribution of a conserved tracer (i.e., CH_4) within the jet for prescribed values of $x/l_b \gg 1$. In the second series, measurements were made at the same downstream location to determine bulk mean values of nitrogen dioxide, the product of the slow reaction.

Assuming that the ratio $[NO_2]/[NO] \ll 1$, values of bulk mean nitric oxide concentration [NO] were determined by the measurement of methane dilution within the deflected jet since $[NO]/[NO]_o = [CH_4]/[CH_4]_o$ as shown in Eq. 32. Hydrocarbon profiles also provided data for the determination of the turbulent parameter γ discussed earlier. A typical asymmetric methane profile is shown in Table 1 where each entry represents the CH_4 concentration at the center of a square sample area of 9 cm^2.

Values of the turbulent parameter $\gamma = (\overline{[CH_4]})^2/\overline{[CH_4]^2} = (\overline{[NO]})^2/\overline{[NO]^2}$ were determined from the hydrocarbon profiles where the overbars are used in this instance to distinguish between the terms in the numerator and denominator of γ as defined by Eq. 8. The mean values which appear in the definition of γ were computed from the hydrocarbon profiles by the method discussed in the Data Analysis section. Results of these measurements are shown in Figure 8 where γ is plotted vs. distance from the jet exit where the key to the symbols used is given in Table 2. The solid line in Figure 8 which appears to slowly increase in value as $x/l_b \to 0$ represents the best fit to the data. Since the theory assumes that γ is a constant along the axis of the jet, a value of $\gamma = 0.65 \pm 0.05$ is recommended for computations from the data shown in Figure 8. Furthermore, the average value of γ does not appear to vary with the magnitude of the momentum-to-buoyancy length ratio l_m/l_b, Figure 9.

Measurements of the bulk mean concentration of nitrogen

TABLE 1. NORMALIZED DILUTION MEASUREMENTS

$R = 2.37$
$l_m/l_b = 5.04$
$\gamma = 0.676$

Sample Location (cm): 58.0
Initial CH_4 Concentration (ppm): 9000.0
Highest Sample Conc. (ppm): 585.0
Sample Area (cm^2): 9.0

	Horizontal Position (cm)								
	12*L*	9*L*	6*L*	3*L*	CTR	3*R*	6*R*	9*R*	12*R*
27	0.0	0.0	0.0	0.0	0.0	0.0	0.0	0.0	0.0
24	0.0	0.0	0.0	0.0	0.09	0.0	0.0	0.0	0.0
21	0.0	0.0	0.23	0.24	0.32	0.12	0.15	0.12	0.0
z(cm) 18	0.0	0.18	0.44	0.58	0.44	0.34	0.32	0.18	0.0
15	0.0	0.17	0.50	0.84	0.38	0.34	0.39	0.28	0.0
12	0.0	0.08	0.48	1.00	0.27	0.16	0.31	0.22	0.0
9	0.0	0.0	0.10	0.33	0.0	0.05	0.14	0.09	0.0
6	0.0	0.0	0.0	0.0	0.0	0.0	0.0	0.0	0.0

TABLE 2. KEY TO SYMBOLS IN FIGURES 8 AND 9

l_m/l_b \ x/l_b	21.8	41.0	82.0	151.3	164.8	318.7	321.1	597.9	1137.0
0.67	⊕								
2.50		●		◓		◒			
2.54			○						
5.04					⊕				
9.78							⊕		
18.3								⊕	
34.8									⊕

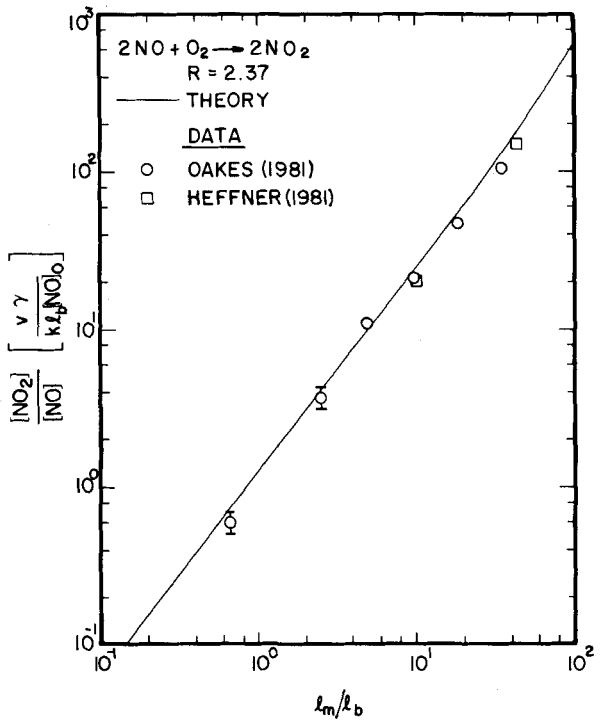

Figure 10. Plot of the end-point conversion Eq. 36 for the oxidation of nitric oxide vs. the ratio of momentum-to-buoyancy length. Initial jet exit conditions are $[NO_2]_o = 0$ and $[O_2]_o \sim 0.21 \times 10^6$ ppm.

dioxide were made in the second phase of the experimental work. The mean values of the concentration of NO_2 were determined from a grid of data points with the same techniques used for methane measurements and for the same jet exit conditions. The $[NO_2]$ data were also measured at the same location x/l_b used for the determination of CH_4 dilution downwind from the jet exit. These results, combined with the previous measurements of tracer dilution and the parameter γ for prescribed jet exit conditions, provide empirical values of the normalized conversion ratio. The above data are plotted in Figure 10 where the solid line was determined from Eq. 36. The agreement between theory and experiment as presented in Figure 10 is excellent. The data are correlated to within 15% of the theory with very little scatter.

Acknowledgments

The research was supported in part by the Department of Natural Resources of the State of Georgia (L.A.O.) and with contributions from the Georgia Tech Research Foundation and DOE grant EE-77-S-02-4319 (L.J.F).

NOTATION

$\mathcal{A}$ = cross-sectional area of jet (m^2)
$[A],[B]$ = bulk mean reactant concentration (ppm)
$[AB]$ = bulk mean product concentration (ppm)
a = dimensionless quantity $[= 2(\eta^2/R)(l_b/l_m)]$
b = transverse length scale of jet (m)
c = dimensionless quantity $[= 1/R\ (l_b/l_m)^2]$
E = relative error
f = dimensionless correction factor
F = buoyancy flux $(= ub^2g(T - T_\infty)/T_1)(m^4\ s^{-3})$
g = gravitational constant $(m{\cdot}s^{-2})$
k_o = rate constant $(= 1.3 \times 10^{-11}\ ppm^{-2}\ s^{-1})$
k = rate constant $(= 2k_o[O_2]_\infty)(ppm^{-1}\ s^{-1})$
l_b = buoyancy length scale $(= F_o/v^3)(m)$
l_g = dimensionless quantity $[= \log_{10}(l_m/l_b)]$
l_m = momentum length scale $(= b_oR)(m)$
q = initial jet volume flow $(= \pi b_o^2 u_o)(m^3{\cdot}s^{-1})$
R = speed ratio $(= u_o/v)$
r = distance along jet radius (m)
s = distance along jet centerline (m)
T = absolute temperature (K)
u = characteristic jet velocity $(m{\cdot}s^{-1})$
u_r = local time-averaged radial jet velocity $(m{\cdot}s^{-1})$
u_s = local time-averaged axial jet velocity $(m{\cdot}s^{-1})$
v = crossflow velocity $(m{\cdot}s^{-1})$
x = horizontal distance downwind of jet exit (m)
y = dimensionless variables $(= s/l_b)$
z = vertical distance from jet exit (m)

Greek Letters

Δ_2 = product formed in near field $x/l_m < 1$.
Δ_1 = product formed in far field $x/l_b > 1$.
γ = dimensionless quantity
α = tangenital entrainment parameter $(= 0.11)$
β = normal entrainment parameter $(= 0.6)$
ρ = bulk mean fluid density $(kg{\cdot}m^{-3})$
θ = angle between horizontal and jet axis (radians)
Ω = dimensionless quantity $[= 2\eta(l_b/l_m)^{1/2}]$
η = dimensionless quantity $\{= [R(\alpha R + \beta)]^{1/2}\}$
λ = dimensionless quantity $[= (\alpha + \beta/R)^{-1/2}]$

Subscripts

o = jet orifice
∞ = ambient

APPENDIX: PERTURBATION EXPANSION OF END-POINT CONVERSION RATIO

Here, we seek a perturbuation expansion of Eq. 36 which is valid in the limit as $l_m/l_b \to 1$. Letting $l_m/l_b = 1 + \epsilon$ where $\epsilon \ll 1$, Eq. 36 is written as

$$\frac{[AB]}{[A]}\frac{u_o\gamma}{klb[B]_o} = f(l_g)\left(\frac{12}{\beta^2}\right)^{1/3}\left(\frac{l_m}{l_b}\right)^{5/3}\left(1 + \frac{\Delta_2}{\Delta_1}\right). \tag{A1}$$

Since $\log_{10}(l_m/l_b) = 0.435\ ln\ (1 + \epsilon) \simeq 0.435\ \epsilon$ for $\epsilon \ll 1$, $f(l_g) = f(\epsilon)$ in Eq. 36, where to first order in ϵ

$$f(\epsilon) \sim 0.79 - 0.246\ \epsilon. \tag{A2}$$

In addition, to first order in ϵ

$$(l_m/l_b)^{5/3} \sim 1 + \frac{5}{3}\epsilon. \tag{A3}$$

Finally, expanding Δ_2/Δ_1 for small ϵ, one has to first order

$$1 + \frac{\Delta_2}{\Delta_1} \sim 1 + \frac{R}{\eta}\left(\frac{\beta^2}{12}\right)^{1/3}\left(1 - \frac{2}{3}\epsilon\right). \tag{A4}$$

TABLE A1. VALUES OF $h(\lambda)$ AND $g(\lambda)$ FOR $\beta = 0.6$, $\alpha = 0.11$

R	λ	$h(\lambda)$	$g(\lambda)$
1	1.19	3.46	1.18
2	1.56	3.75	1.14
5	2.08	4.16	1.10
10	2.44	4.44	1.07
20	2.70	4.65	1.05
∞	3.03	4.91	1.03

Multiplying Eqs. A2, A3 and A4 and retaining only first-order terms, one finds for $\beta = 0.6$ that

$$f(l_g)(l_m/l_b)^{5/3}\left(1+\frac{\Delta_2}{\Delta_1}\right) \sim h_1(\lambda)(1+\epsilon g(\lambda)) \qquad \text{(A5)}$$

where $g(\lambda) = 1.35\,(1 + 0.16\lambda)/(1 + 0.31\lambda)$, $h_1(\lambda) = 0.79 + 0.245\lambda$ and $\lambda = (\alpha + \beta/R)^{-1/2}$, Table A1. Since Eq. A5 represents the first-order expansion of the power law $h_1(\lambda)(l_m/l_b)^{g(\lambda)}$, as $l_m/l_b \rightarrow 1$ and $(12/\beta^2)^{1/3} = 3.22$, Eq. A1 reduces to the simple form

$$\frac{[AB]}{[A]}\frac{u_o\gamma\,[B]_0}{kl_b} \sim h(\lambda)(l_m/l_b)^{g(\lambda)} \qquad \text{(A6)}$$

where $h(\lambda) = 2.53\,(1 + 0.31\lambda)$.

LITERATURE CITED

Brodkey, R. S., Ed., *Turbulence in Mixing Operations*, Academic Press (1975).

Escudier, M. P., "Aerodynamics of a Burning Turbulent Gas Jet in a Crossflow," *Comb. Sci. and Tech.*, **4**, 293 (1972).

Fay, J. A., "Buoyant Plumes and Wakes," *Ann. Rev. Fluid Mechanics*, **5**, 151 (1973).

Fischer, H. B., E. J. List, R. C. Y. Koh, J. Imberger, and N. H. Brooks, *Mixing in Inland and Coastal Waters*, 346, Academic Press (1979).

Forney, L. J., "Turbulent Plume in a Laminar Crossflow," MS Thesis, MIT, Cambridge, MA (1968).

Forney, L. J., and D. A. Heffner, "Slow Second Order Reactions in a Power Plant Plume: Application to Preliminary Data," *Chem. Engr. Comm.* **17**, 227 (1982).

Forney, L. J., and T. C. Kwon, "Efficient Single-Jet Mixing in Turbulent Tube Flow," *AIChE J.*, **25**, 623 (1979).

Forney, L. J., and Z. G. Giz, "Slow Chemical Reactions in Power Plant Plumes: Application to Sulfates," *Atoms. Envir.*, **14**, 533 (1980).

Forney, L. J., and Z. G. Giz, "Fast Reversible Reactions in Power Plant Plumes: Application to the Nitrogen Dioxide Photolytic Cycle," *Atmos. Envir.*, **15**, 345 (1981).

Freiberg, J., "Conversion Limit and Characteristic Time of SO_2 Oxidation in Plumes," *Atmos. Envir.*, **12**, 339 (1978).

Gouldin, F. C., "Role of Turbulent Fluctuations in NO Formations," *Comb. Sci. Tech.*, **9**, 17 (1974).

Heffner, D. A., "Analytical Expressions for Slow Pseudosecond-Order Reactions in Plumes: Comparison with Experimental Results," MS Thesis, Georgia Institute of Technology, Atlanta (1981).

Hoult, D. P., and J. A. Fay, and L. J. Forney, "A Theory of Plume Rise Compared with Field Observations," *J. Air Pollut. Control. Assoc.*, **19**, 585 (1969).

Hoult, D. P., and J. C. Weil, "Turbulent Plume in a Laminar Crossflow, *Atmos. Envir.*, **6**, 513 (1972).

Lin, C. H., and E. E. O'Brien, "Turbulent Shear Flow Mixing and Rapid Chemical Reactions: an Analogy," *J. Fluid Mech.*, **64**, 195 (1974).

McKelvey, K. N., H. N. Yieh, S. Zakanycz, and R. S. Brodkey, "Turbulent Motion, Mixing, and Kinetics in a Chemical Reactor Configuration," *AIChE J.*, **21**, 1165 (1975).

Morton, B. R., G. I. Taylor, and J. S. Turner, "Turbulent Gravitational Convection from Maintained and Instantaneous Sources," *Proc. Roy. Soc., London*, **A234**, 1 (1956).

Oakes, L. A., "Measurements of Slow Second-Order Reactions in a Buoyant Jet in a Crossflow," Tech. Rep. MSCEGT81-024, Georgia Institute of Technology, Atlanta (1981).

Rajaratnam, N., *Turbulent Jets*, Elsevier Scientific Pub. Co. (1976).

Schwartz, S. E., and L. Newman, "Processes Limiting Oxidation of Sulfur Dioxide in Stack Plumes," *Envir. Sci. Technol.*, **12**, 67 (1978).

Singh, M., and H. L. Toor, "Characteristics of jet mixers—effect of number of jets and Reynolds numbers," *AIChE J.*, **20**, 1224 (1974).

Torr, H. L., "The Nonpremixed Reaction: A + B → Products, Chap. 3," *Turbulence in Mixing Operations*, Ed., R. S. Brodkey, Academic Press (1975).

Wright, S. J., "Effects of Ambient Crossflows and Density Stratification on the Characteristic Behavior of Round Turbulent Buoyant Jets," Tech. Rep. KH-R-36, W. M. Keck Lab. of Hydroaulics, California Institute of Technology, Pasadena (1977).

Manuscript received January 25, 1982; revision received January 28, 1983, and accepted February 9, 1983.

Bubble Formation at Vibrated Orifices: Medium-Chamber-Volume Region

The bubble formation process at small, single, circular orifices at low gas flow rates is modified when the system is vertically vibrated in a sinusoidal fashion.

For systems with significant gas chamber volume, bubble volume in the vibrated case is smaller than in the nonvibrated case. The vibrations increase the amount of liquid weeping through the orifice into the gas chamber. A simple inviscid model adequately predicts bubble formation in the medium-chamber-volume region at low values of amplitude and frequency of vibration and low viscosities. The boundaries of the transition from the $FR \gg 1$ to the $FR = 1$ regions are described in terms of "the acceleration number/Eötvös number."

C. T. BAKER and NOEL de NEVERS

Department of Chemical Engineering
University of Utah
Salt Lake City, UT 84112

SCOPE

Bubbles play a significant role in many important industrial processes, including distillation, gas-liquid chemical reactors, absorption, and flotation. In many of these processes, bubbles are formed by forcing gas through an orifice into a liquid; the principal reason for doing this is to increase the interfacial area between gas and liquid.

The formation of bubbles at single, submerged orifices has

C. T. Baker is presently with Conoco, Ponca City, OK 74603.
Correspondence concerning this paper should be directed to N. de Nevers.